Front Initiation on Microdesigned Composite Catalysts

Xiujiang Li, Ioannis G. Kevrekidis *

Department of Chemical Engineering, Princeton University, Princeton, NJ, 08544

Michael Pollmann, Athanasios G. Papathanasiou, and Harm Hinrich Rotermund

Fritz-Haber-Institut der Max-Planck-Gesellschaft, Faradayweg 4-6, 14195 Berlin, Germany

(March 8, 2002)

Abstract

We first briefly review the subject of spatiotemporal pattern formation on microdesigned composite catalysts. One of the most significant interaction mechanisms between different reacting domains (consisting of different metal catalysts such as Pt and Rh, coupled through surface diffusion) is the initiation of reaction fronts at the interface between them. We then explore in some detail the effect of two-dimensional composite geometry on this basic building block of composite catalyst dynamics.

Spontaneous pattern formation in nonequilibrium systems is a topic of intense current research in many fields, ranging from catalysis and fluid mechanics to developmental biology. The common mathematical underpinnings of the fascinating and complex phenomenology observed allows for information gleaned from model problems in one discipline to lead to insights in completely different disciplines; CO **oxidation on Pt single crystals (and several other catalytic**

to whom correspondence should be addressed, yannis@princeton.edu

reactions) have become such paradigms over the last decade. As the essential features of pattern formation in uniform media are gradually understood, the effect of medium heterogeneities on the phenomenology (in different terms, the "robustness" of the phenomenology to imperfections in the medium) is becoming the focus of many efforts. The construction of active media decorated with precisely designed heterogeneities is a cornerstone of this research: it is the basis for the systematic exploration and (along with computational studies) understanding of the effect of heterogeneities on the overall spatiotemporal dynamics. This article summarizes research on microdesigned composite catalysts in our group over the last several years, and presents new results highlighting the effect of the geometry (size, curvature) of active heterogeneities on the overall catalytic dynamics.

I. INTRODUCTION

Many heterogeneous catalytic reactors exhibit rich nonlinear dynamic behavior over some region of their operating parameter space. This richness extends across scales and reactor types, all the way from the macroscopic scale (e.g. the "textbook" CSTR[1] and tubular reactor models[2], as well as modern reverse flow reactors[3]) and the "mesoscopic" one (e.g. single metal crystals in high vacuum conditions) to even the nanoscale (e.g. catalytic oscillations on FEM tips[4]). In all of these problems, the intimate coupling of reaction with transport lies at the core of the observed behavior. Transport appears in many forms: from bulk flow and dispersion in the large scale reactors and pore diffusion in permeable catalysts, to interphase transport (adsorption and desorption) and surface diffusion on single crystal surfaces.

The fact that the catalytic medium is not homogeneous is also a feature that persists across scales: a packed bed is comprised of many individual pellets (typically cm or mm size), while a polycrystalline foil or wire surface is composed of polycrystalline facets ($\approx$100 micron size) and even single crystal surfaces have defects and microfacets (at the nanometer scale). In most routine modeling work, and at the level of reactor-scale (e.g. overall rate information) these heterogeneities are averaged out, and their effect is contained in the slightly modified *effective* overall transport and kinetic coefficients in the macroscopic equations of change. Understanding catalytic mechanisms, however, often requires taking these heterogeneities into account[5,6]; and there are cases in which their effect in the overall behavior goes beyond just a slight modification of an effective coefficient in the macroscopic equations. One of the most striking such effects, that has been extensively studied recently, is the pinning of fronts in discrete media[7,8]. One of the most studied heterogeneous reacting media in the current dynamics literature is heart tissue[9,10].

When we embark on a systematic exploration of the effects of heterogeneity on overall dynamics (and, in particular, in this paper, on heterogeneous catalytic dynamics on metal crystal surfaces at vacuum conditions) modeling has a new component: in addition to reaction and transport, we need to model heterogeneity also - both its geometry and its "intensity". This modeling can be done in two ways: first, we can measure experimental heterogeneities (either in detail, or in statistical fashion) and then create *on the computer* media that have either exactly the same heterogeneities or heterogeneities that are similarly distributed. On the other hand, we can *experimentally* create model media that have a designed and carefully controlled heterogeneity pattern, and perform experiments in such media; this would allow us to experimentally test theoretical/computational predictions in a controlled way. Beautiful chemical engineering examples of this "reverse" approach, that is, the construction of experimental media with perfectly controlled heterogeneities, can be found in the work of the Scriven group for trickle bed hydrodynamics[11], and of the Payatakes group for flow in porous media[12].

The fabrication and study of microcomposite catalysts (single crystal catalytic surfaces decorated with controlled heterogeneity fields) started in our group in 1993[13]; Prof. M. Graham of the University of Wisconsin, then a postdoctoral fellow in the group, played a key role at that time. The original motivation was a pure modeling one: there was a clear need for quantitative comparisons of modeling and simulations with the spectacular spatiotemporally resolved measurements from photoemission electron microscopy (PEEM)[14]. Since the scale of the typical experiment was 1cm, and the scale of a typical pattern was 10 microns, a multitude of patterns, sometimes affected by crystal imperfections, were competing on the catalyst surface. The necessity then arose for isolating building blocks of the spatiotemporal dynamics (single pulses, single spirals, single fronts) in domains of size and nature commensurate with the object of the study. Narrow circular corridors (simulating one-dimensional media with periodic boundary conditions for pulses), as well as square and circular domains with variable dimensions (to study isolated spirals) were constructed using microlithography on Pt single crystal surfaces. Since the study focused on the effects of geometry and size, the boundaries of the domains were chosen to be inert, 2000 Å tall titanium walls, presumed to implement what in the modeling are no flux boundary conditions (Fig. 1). An array of experimental and concomitant computational studies ensued: the study of the effect of domain size on spiral rotation speed[15], and the study of the effects of curvature and anisotropy on chemical pulses[16–18] are representative examples of this research. Dr. M. Bär, of the MPIPKS in Dresden, then also a postdoc in the group, and Dr. A. Bangia, then a graduate student, were mainly responsible for our group's modeling work at the time. It is important to note that computational studies of the effect of complex geometry on pattern formation well predated our experimental and modeling work on CO oxidation. Effects of geometry on pattern formation had long been studied in problems such as the Faraday experiment[19] (and its whimsical "patterns in France" realization). On the reaction-diffusion side, a remarkable achievement was the printing of structured catalyst membranes for the BZ class of reactions by Schowalter in 1995[20]; we also know that illuminating the photosensitive BZ through etched glass plates of different symmetry (stripes, hexagons) was used to drive the experiments towards the corresponding steady states in the Swinney group in Austin. These experiments were, no doubt, the precursors of the current experimental spatiotemporal forcing work in Austin[21], using a digital projector to spatiotemporally drive the system. Many other interesting studies have appeared in the literature since 1990 studying the effect of geometry on reacting pattern formation; examples of this work include papers by Agladze et al.[22], Forsterling et al.[23], Suzuki et al.[24] etc. It is also worth mentioning that at around the same time -in the early 90's- the field of microreactor engineering virtually exploded, providing a new bridge between chemical dynamics and microelectronics fabrication, and opening many new avenues and possibilities for technological development[25,26].

The first lithography mask we constructed in the summer of 1993 included, among other patterns, a lattice of inert Ti inclusions in a "field" of Pt. The patterns that emerged covered a spectacular range: depending on experimental conditions, pattern formation could proceed as if the lattice of obstructions was not there; or -conversely- the lattice of obstructions would completely determine the wavelength and nature of overall pattern formation. This clearly shows that geometry is much more than just as a "focusing" tool for studying pattern formation by isolating features so that they can be studied systematically: it is actually a way to "talk to" the physical processes, affect them, in a sense drive or control them. Microlithography allowed us to do this at a scale (microns, tens of microns) commensurate with the spontaneous pattern size - a regime where one might expect the most "resonance" between domain size and spontaneously forming patterns.

At the same time, it was clear that "geometry" does not have to be inert. Instead of decorating the surface with a lattice of inert heterogeneities, it is possible to deposit on it a lattice (or other patterns) of *active* heterogeneities - different catalytic metals (See Fig. 2 for an example). Over the last several years we have created composites combining Pt and dispersed Au[27], Pt and Rh, Pt and Pd, Pd and Rh as well as Pt and CeO_2 domains[28–33]; recently, for the first time, we constructed tricomposite patterns (Pt, Rh and TiO_2). We have also constructed metal-oxide composites by depositing Pt and Pd on sapphire (Al_2O_3) windows, to study spillover effects. These "reactive patches" communicate through the gas phase, but -more importantly for our studies- they communicate through surface diffusion at the interface between them; the shape and extent of this interface is something that we can control by construction of the catalyst. We must of course bear in mind that some alloying always occurs at the interface between composite patches; careful studies have shown that, at least in one case, the range of the alloying extends over approximately only 2 micrometers.

The phenomenology of pattern formation in such media is even richer and more bewildering than pattern formation in uniform media; simulations by many groups[34–36] (including ours[37,15,16,38–44]) have only started to sample what is possible. From this wealth of phenomenology we single out here one mechanism in two guises: "leaky walls" and front initiation (see Fig. 3). The "leaky wall" effect is illustrated in Fig. 3(b) ; corridors of Pt are surrounded by Rh, which (by adsorbing CO more easily) is believed to act as a CO reservoir for the Pt. Oxygen pulses in the Pt corridor are observed to be triangular rather than rectilinear; this is qualitatively modeled[32] as the result of lateral flux of CO from the Rh surroundings onto the Pt corridor. Front initiation in bistable composites, studied in detail in the Thesis[45] and in[42,44], is the subject of our new results section below.

As pattern formation in homogeneous media becomes better understood, heterogeneous media increasingly become the focus of experimental and computational work. In heterogeneous catalysis, nanolithography has been used to construct composite catalysts (e.g. Ag/Si, Ag/Al and Pt/Si) for partial oxidation reactions by the group of Somorjai[46] as well as Delmon and the late J. Block[47]. At the same time, experimental and computational work on a variety of systems and their models is in progress (see for example[48,49]).

An important point, to which we will return in our closing remarks, is the study of spatiotemporal forcing of pattern formation. *Temporal* forcing of chemical reactions, for example periodic variation of a global quantity like temperature or partial pressure of reactant *uniformly in space*, has long been considered as a possible path towards improving reactor performance. Composite catalysts could be considered as *spatially* structured -but uniform in time- forcing: heterogeneity is the way we try to affect the reaction, its shape in space is determined on construction, and it remains constant over the operational life of the catalyst. Spatiotemporally forced systems, in which many exciting discoveries have been made recently[50], can in fact be thought of as *temporally varying composites*: composites whose geometry and shape change as a function of time. Such studies in open as well as in closed loop[51,21,52] constitute a current frontier in pattern formation, resonating with mathematical issues of systems theory and control, homogenization, as well as stochastic PDEs.

We started with a brief review of studies of nonlinear dynamics and pattern formation on microdesigned heterogeneous catalytic surfaces, and with a glimpse of comparable studies in structured reaction-diffusion media. In the remainder of this paper we will focus on a particular phenomenon, which constitutes a fundamental "building block" of composite surface dynamics: the initiation of fronts (e.g. ignition fronts) at the interface between two surface "patches". We will present an array of new results exploring the effect of geometry (boundary curvature in two dimensions) on this phenomenon, both computationally and experimentally. We will mention (and show just a glimpse) of the effect on this phenomenon of anisotropy, and conclude with a discussion of future research directions, including the recently constructed addressable catalyst surfaces[50], on which the heterogeneity fields can be controlled spatially *and* temporally.

II. MODELING AND COMPUTATION

A. Modeling front initiation in one and two dimensions

Computational and experimental studies of the phenomenon of front initiation at the interface between components of a microcomposite catalyst surface have appeared in[42,44]. The experiments involved the $NO+H_2$ and the $NO+CO$ reactions on Pt/Rh as well as Pt/TiO_2 microcomposite catalysts; the experimental composite geometry consisted of circular inclusions of one catalyst in a plane of the other. The modeling was done in one spatial dimension (stripes of one catalyst in the other), or effectively in one spatial dimension (circular inclusions, modeled axisymmetrically). Our modeling effort in this paper will focus on truly two-dimensional inclusions. We start, however, by presenting the basic results of the one dimensional case, since we want to later contrast them with the fully two-dimensional case. Our illustrative kinetics will come from a simplified single species model of NO reduction :

$$\begin{aligned} &NO + * \leftrightarrow NO_{ads} \\ &NO_{ads} + H_2 + 2* \rightarrow H_2O + \tfrac{1}{2}N_2 + 3* \end{aligned} \tag{1}$$

where * represents the empty sites on the surface. The model equation is:

$$\frac{\partial C}{\partial t} = D\nabla^2 C + k_a(1-C) - k_d C - k_r(1-C)^2 C \tag{2}$$

where C denotes the NO_{ads} coverage, k_a, k_d and k_r are the rate constants of adsorption, desorption and surface reaction, respectively.

We chose this model for its simplicity, and because we believe it embodies the "minimum requirements" (that is, bistability) for rationalizing the phenomena we have observed in NO reduction as well as in CO oxidation. The experimental results in the rest of the paper will be on CO oxidation. Modeling them *semi-quantitatively* would require computations with at least three coupled PDEs (for the coverages of CO, O and the degree of surface reconstruction, based on the kinetic model of Krischer et al.,

$$\begin{aligned}
\tfrac{\partial u}{\partial t} &= k_u s_u p_{CO}[1-(\tfrac{u}{u_s})^q] - k_d u - k_r uv + D_u\nabla^2 u \\
\tfrac{\partial v}{\partial t} &= k_v p_{O_2}[s_{v1}w + s_{v2}(1-w)](1-\tfrac{u}{u_s}-\tfrac{v}{v_s}) - k_r uv \\
\tfrac{\partial w}{\partial t} &= k_p(f(u)-w)
\end{aligned}$$

where u, v and w refer to the surface coverage of CO and O and the fraction of the reconstructed surface, respectively. The description and the values of the various constants can be found in reference[53]); or possibly two PDEs in an approximate reduced model arising through the adiabatic elimination of the relatively fast O coverage equation[54]. Tripling the number of unknowns in a truly two-dimensional (and three-dimensional when time-dependent behavior is computed) problem would make the computations considerably more unwieldy. Since additional features of the problem are not yet quantitatively known (e.g. adsorption kinetics and diffusivity for CO on a few hundred Å of evaporated Rh on Pt), we decided to perform the computations on this simplified model of NO-reduction. We believe that, at the level of qualitative understanding sought in this paper, these computations assist the reader (as they assisted us) in rationalizing and even predicting most of the observed phenomenology.

Geometry: Fig. 4 is a photograph of a portion of the surface of our microcomposite $Pt-Rh$ catalyst. Fig. 5 shows the two composite geometries (unit cells) we will model: a two-dimensional rendition of the one-dimensional problem (Fig. 5a), and the fully two-dimensional rhomb-inclusion problem (Fig. 5b), including the equations and boundary conditions. Adsorption, desorption and reaction as described in Equ. 2 (different constants on the different catalytic components A and B) take place along with (isotropic) diffusion on the composite surface. The diffusion coefficients can also, in principle, be different; in these qualitative simulations we have used the same diffusivity for the two metals. The boundary conditions come from symmetry (no flux around the boundary of the unit cell in both one and two-dimensions) as well as diffusive coupling (normal fluxes on both sides of the A-B interface are equal, and the chemical potential of the adsorbate is continuous) at the (idealized) interface. The latter condition yields a nonlinear algebraic equation to be solved at the boundary, turning the discretized problem into a set of coupled, nonlinear differential-algebraic equations (DAEs).

Numerics: The problem is discretized through the finite element method. Typically of the order of 100 linear elements in one dimension and 3000 bilinear elements in two dimensions are used; the convergence of the results has been confirmed both through higher order elements (Hermite cubics in 1D, biquadratics in 2D), as well as with the FEMLAB commercial package. The steady state bifurcation diagrams we will show have been computed through pseudo-arclength continuation and full Newton iteration with a frontal direct solver. The time-dependent results were obtained using a sufficiently resolved implicit Euler method, and they have also been confirmed through DASSL. Stability results, when reported, have been deduced from integration and occasionally quantified through linearization (a generalized eigenproblem, solved through ARPACK[55]).

B. Some Computational Results on Front Initiation

One-dimension: striped composite. Fig. 6 is a representative compendium of one-parameter bifurcation diagrams for the composite stripe geometry, which we solve as a one-dimensional problem. The parameters of the computation are included in the caption;

we study what happens on two stripes of equal length and equal diffusivity, but of different kinetic parameters as a function of (a) kinetics (reaction rate constant) for various (b) geometries (stripe length). At large lengths, we see the expected (from[42]) asymptotic behavior: there exist three basic stable branches: one where none of the two stripes is "ignited" (we call this the (-,-) branch); one where the more active of the two branches is "ignited" while the less active is not yet (the (+,-) branch); and finally one where they are both ignited (the (+,+) branch). These stable branches are connected through turning point bifurcations and practically vertical branches in the bifurcation diagram. The right inset in the figure shows representative spatial profiles of the solution for points along the rightmost vertical branch. These solutions clearly correspond to fronts which, starting at the interface between the two catalytic components "sweep" the less active catalytic component (A), igniting it. It is interesting to observe how this asymptotic figure gets gradually modified as the length of the stripes gets smaller and smaller, and the solution can no longer be identified with sharp, infinite-medium "fronts" (see the left inset).

Two-dimensions: rhomb inclusions. Fig. 7 shows the bifurcation diagram (again as a function of reactivity) of a single two-dimensional composite (a rhombic inclusion in a square unit cell, whose dimensions are given in the figure caption). This figure in effect summarizes the message of our paper: the picture shares many qualitative features with the one-dimensional diagram. We can again identify a (-,-), a (+,-) and a (+,+) branch. In this case, the more active component is on the outside of the rhomb. Let us concentrate on the (-,-) to (+,-) ignition. Instead of a single vertical branch (that we observe in the one-dimensional case) we observe here a "jungle" of branches more or less in the same parameter range. These branches all correspond to qualitatively similar solutions, in which the active component (the complement of the rhomb) ignites through a front that sweeps it (see the inset in Fig. 7 and the corresponding solution portraits in Fig. 8). What distinguishes these solutions from each other ? The answer, very qualitatively, is geometric freedom: the practically neutral ignition front has essentially but a single degree of freedom in one dimension - its distance from the material interface. A delicate balance ensues between the system parameters (that tend to make the front move) and the distance from the interface (that breaks the translational invariance); this balance determines the eventual distance of the front from the interface, as well as its ultimate shape.

In two dimensions, however, this distance is not just a single number but a function: the distance of the front from a rhomb heterogeneity varies along the front perimeter. A third player (front curvature) also plays an important role; the delicate balance between parameter values, front curvature and front shape determines now the final steady front. This balance can sometimes successfully close in more ways than one; the ignition front can rearrange not only its position, but its entire shape. The solution snapshots in Fig. 8 , which only show the onset of the ignition front, clearly appear similar, and only have their "hot spots" at slightly different places. One might ask, why is there no comparable "jungle" at the (+,-) to (+,+) ignition ? The answer, briefly, is that the inclusion (which gets ignited there) is too small to sustain practically neutral asymptotic fronts that easily translate and deform, the underlying cause of these "branch jungles".

Consider now the flip side: the active component is the small inclusion. In this case (Fig. 9) it is the (-,-) to (+,-) ignition that has no vertical branch; the almost neutral asymptotic fronts occur when the large complement of the inclusion ignites, at the (+,-) to (+,+) transition. This is why now the "branch jungle" occurs at this latter transition. Fig. 10 is a blowup of a portion of this almost vertical branch, and the insets show snapshots of the solution on a few of these "secondary" branches. We have chosen to include these for two reasons: first, the "geometric freedom" of the front in two dimensions, allowing it to "ripple" is manifest. Another important point, for the bifurcation minded reader, however, is that in this plot, a number of perturbed pitchfork bifurcations can be seen. The reason for these perturbed pitchforks is that the inclusion is not symmetric: it is a rhomb rather than a square; if the inclusion was square, many of the bifurcations leading to the "branch jungle" would have been symmetric pitchfork bifurcations. Here the square symmetry has been broken by construction of the inclusion, but a "memory" of the symmetric picture remains in the relative disposition of the various solution branches.

III. EXPERIMENTAL RESULTS AND COMPUTATIONAL COMPARISON

A. Experimental Techniques

Guided by the initial experiments reviewed above, and to some extent by the modeling, we decided to study this problem through a different reaction: The oxidation of CO in the 400-480 K temperature range for a partial pressure of oxygen of 4×10^{-4} mbar and for CO-presssures in the 10^{-5} mbar range. Here we report new experiments obtained on composite surfaces created by standard microlithographic deposition of two different metals (Ti, Rh) on a Pt(110) single crystal substrate; the patterned layers were typically 1000 Å in height. For the sample crystal we constructed, stripe, square and rhomb inclusions of various sizes and angles (180° for the stripes, 90° for the squares, as well 30° and 60° degrees for the rhombs) (see Fig. 4). Furthermore, we constructed both "positive" and "negative" rhombs (that is, Pt rhomb inclusions in Rh(Ti) as well as Rh(Ti) rhomb inclusions in Pt.).

The real-time measurements were made using photoelectron emission microscopy (PEEM)[14], whose signal is directly correlated with the local work function of the surface. On the clean Pt(110)-surface O-covered regions appear dark because of the high dipole moment of O-atoms, increasing the work function. CO-covered Pt(110) regions appear gray in in PEEM-images. To avoid intense alloying at the metal-metal interfaces (known to extend, under different conditions over as much as 2 microns from the interface), the preparatory sputtering/annealing cycles were not carried above 700 K.

B. Phenomena: experiments and qualitative modeling

It is already known, from the axisymmetric data of reference[42], that curvature, -a truly two-dimensional feature- can play a significant role in front initiation at composite interfaces. We use a sequence of composite inclusions (rhombs) with varying angles as a means to systematically parametrize the effect of gradual increase in curvature. In what we will show below, both computationally and experimentally, it is convenient to think that we start on the (+,-) branch, and, by making conditions gradually more intense, we study the (+,-) to (+,+) ignition; doing this for different rhomb angles will then bring out the effect of curvature. In the simulations, the "more active" medium was taken to be an already ignited bistable one; in the experiments this role was played by Rhodium, which, through the supply of additional surface CO, "catalyzed" the ignition of the Pt domains.

Fig. 11 shows experimental results of a transient that spans the ignition. We begin (Fig. 11(a)) at an oxygen covered ($P_{CO} = 0$) steady state, where the Pt rhomb inclusions appear dark; P_{CO} is then ramped to $3 * 10^{-6}$mbar, a value at which the steady state is "ignited", that is, CO-covered (PEEM-light, Fig. 11(e)). It is interesting to observe how the transition proceeds dynamically: the outside "active" Rh immediately becomes CO covered (Fig. 11(b)); the Pt "ignition front" (light color) starts invading the rhombs from their sharper angles (Fig. 11) and only later in time do we have light color at the wider angles, eventually sweeping the Pt domain. The fact that inclusions with several different angles are observed in the same microscope image allows us to see that the sharper rhombs become ignited faster, and that at steady state (Fig. 11(e)) they are completely ignited. A qualitative reproduction of this transient is provided through our computational caricature in Fig. 12. Here again, following a step change in parameter beyond the (+,+) ignition, the rhomb inclusion starts getting ignited at the sharp angles, and the front proceeds inwards, eventually covering the entire domain.

Clearly, geometry, through boundary angle sharpness, plays a role in dynamic front initiation. Fig. 13 shows experimentally that -as one might expect- it also plays a role in the formation of stationary fronts. The experimental conditions are included in the figure caption, and we have used pseudocolors to enhance the grayscale experimental PEEM data. It is clear that -as P_{CO} is gradually raised- sharp corners nucleate first (again notice that these are steady state, not transient, results); and that the displacement of the steady front from the boundary (the degree it has progressed in the Pt domain) is larger at larger P_{CO}. This can be rationalized if we consider that the basic mechanism involved is the diffusion of additional CO from the Rh to the Pt: it is clear that the influx of CO per unit Pt area is larger at sharp angles (more Rh, less Pt) than at wide angles (less Rh, more Pt).

Fig. 14 quantifies this through modeling. It contains the bifurcation diagram (in the neighborhood of the (+,+) ignition) of our caricature for three different geometries, all of the same area, whose angles (30°, 60° and 90° degrees) were chosen to be the same as in the experimental results we just discussed. The insets show pseudocolor snapshots of the solution at three different conditions, so that the effect of geometry (angle) is underscored. It is clear that front nucleation occurs earlier for the sharper angles. It is also interesting that, for this model, beyond the nucleation and gradual displacement of stationary fronts, actual ignitions (turning point bifurcations) are part of the story. The sharper inclusion not only nucleates first, but actually also "jumps" (becomes fully ingnited at a turning point) first. This gives rise to conditions (last column in the inset) where the sharp rhomb inclusion is fully ignited, while the wider angle ones are nucleated but not yet fully ignited.

We now turn to the "flip" case: the active component is inside, and nucleation and propagation of fronts occurs "away from" the rhombs. Fig. 15 shows experimental results (raw data and pseudocolor enhancement) of CO fronts nucleating at Rh inclusion boundaries towards the surrounding Pt areas. In this case it is observed (and can also be easily rationalized) that the fronts will nucleate first at the wide angles (more Rh, and less Pt); actually, the nucleation should start earlier for 180° degrees, that is, for the parallel sides of the inclusions. It can be clearly seen that the wide angles and parallel sides have nucleated CO fronts, while the sharper angles have not. The lack of nucleation is more pronounced the sharper the angle is: 90° degree angles (squares) have nucleated CO fronts all around them, while the 60° and 30° degree angles have not. This is computationally confirmed in Fig. 16: fronts again are seen to nucleate first at the wider angles and parallel inclusion sides. The conditions for the computation are contained in the figure caption.

We conclude the results section by pointing out yet another feature of two-dimensionality that can play a significant role in composite dynamics: anisotropy. In the results we showed here, all two-dimensional computations had isotropic diffusion, and the discussion of the experimental results did not get drastically affected by anisotropy. There are cases, however, where anisotropy can play an important role, above and beyond the one played by composite geometry. Fig. 17 confirms this statement: depending on how two equal size and angle rhomb inclusions are oriented regarding the crystal lattice principal axes, front nucleation and ignition can be quite different. For these experimental conditions, nucleation is faster at sharper angles, since Rh is on the outside; this is clear in both Fig. 17(a) and (b). Nucleation, however, is much more pronounced when the favored sharp angles are more or less aligned with the fast lattice diffusion axis. In Fig. 17(b), the less favored 120 degree angles have not nucleated yet. Anisotropy is a very important player in spatiotemporal pattern formation[56,57].

IV. SUMMARY AND DISCUSSION

We briefly discussed our studies, over the last eight years, of microstructured and microcomposite catalysts. Initially this effort was motivated from modeling considerations: to analyze and understand certain reaction-diffusion phenomena, we wanted to build the "minimal" geometries (such as quasi-one-dimensional rings for pulses) which would allow us to in some sense "isolate" the phenomenon of interest, study its parametric dependence, and compare it with modeling systematically. What started as a "focusing" tool for the study of individual building blocks of nonlinear dynamic behavior, however, quickly turned into an exploration tool. We constructed surfaces of designed geometric complexity: regular lattices of heterogeneities, and domains with complex geometric features and boundary curvatures were immediately studied. *Active* composite surfaces, where more than one catalytic components are deposited in a regular pattern next to each other, and are coupled by surface diffusion, was also immediately attempted. The prospect of optimizing (or, to begin with, affecting) reactor performance, especially selectivity in complex reaction pathways through composite geometry design has always been a driving force for our work. While encouraging initial theoretical results have been obtained, this goal remains elusive; to some extent this is due to the fact that the reactions mostly studied by the group are relatively simple in terms of reaction pathways. This direction is still being pursued.

It is worth mentioning at this point that the experimental and modeling work associated with microstructured and microcomposite catalysts presents the opportunity for very strong synergism with a number of branches of applied mathematics. There is, of course, the obvious connection with scientific computation and numerical bifurcation theory; but in addition, this work is provides a wonderful application field for homogenization and effective medium theory[58]. There has been extensive research recently on the propagation of pulses and fronts in composite and discrete media (see the recent review by Xin[59] as well as the beautiful work of Keener[7,8]). There has also been extensive work on novel scientific computation techniques that are particularly applicable for coarse/multiscale computations in media with microstructure; we note the recent work of Tom Hou[60,61], the approach of Rob Phillips[62], as well as the wavelet based homogenization work of Beylkin[63], Engquist[64], Gilbert[65]. A wavelet based numerical homogenization approach for pattern formation in composite reactive media has recently been implemented by our group[66]. Homogenization computations for the CO oxidation problem on composite catalysts can be found in[67], see also[68,69]; a new computational approach to "on the fly" homogenization using time-steppers is illustrated with a CO oxidation model example in reference[70]. Composite geometry optimization with an overall performance objective, real time image processing, and systems theory applications (distributed nonlinear observers, hierarchical control schemes) are some areas of applied mathematics which can play a role in advancing our understanding of composite catalysts. We believe that these fields can in turn greatly benefit, both in terms of validation and in terms of new questions posed, by composite catalyst experiments and modeling.

One truly exciting recent development is the successful implementation of what we term an "addressable catalyst surface"[50]. The new element is a focused laser beam, which is computer controlled, and can raster the surface -or follow any other desired spatiotemporal path on it- through a pair of galvanometer mirrors. As the laser beam sweeps the surface, the local temperature temporarily rises by a few degrees (the extent and duration of the temperature rise depends on the laser power and speed, as well as on the properties of the metal crystal). We can therefore write temperature patterns on the surface “at will”; these patterns could be constantly refreshed (in which case we have a constant field of temperature heterogeneity, or a “temperature composite”) or they can vary in space and time in a prescribed manner (a “spatiotemporal composite”). This development opens a new set of possibilities in affecting catalytic spatiotemporal dynamics: “talking to” the reaction not only in space (as a composite does) but in both space and time; it has even been possible to close the loop between distributed sensing and the laser beam through real time image processing, and thus acquire a distributed control system.

The effect of heterogeneity fields in physicochemical processes (and in pattern formation in particular) is taking center stage in many disciplines, as the processes of interest become more and more microscopic. A few recent efforts include the use of templates to aid the self-assembly of diblock copolymer[71]; polymer phase transitions in confined geometries[72]; inkjet catalyst printing to catalyze electroless deposition of electronic circuit lines[73]; and “geometric control of cell life and death”[74,75]. Along the lines of “spatiotemporally heterogeneous” media, it is worth noting the recent results of Aksay and coworkers, who use light fields to assemble colloidal crystals[76].

Heterogeneous catalytic patterns have become, over the last decade, a model system for nonequilibrium pattern formation across disciplines. Microstructured and microaddressable catalytic surfaces, in addition to the insights and possibilities they open in surface science and heterogeneous catalysis, may well be able (because of the relative ease of construction, real time imaging and addressability) to assume a comparable “model system” role for dynamics in heterogeneous media.

Acknowledgements We gratefully acknowledge partial support by the Program for Plasma Science and Technology at Princeton University (X. Li); also by NSF, AFOSR and the Humboldt Foundation (I.G.K.), ONR (H.H.R., I.G.K.) and an E.U. Marie Curie Fellowship (A.G.P.) under contract Nr: HPMFCT-2000-00685. We take this opportunity to mention, with sincere appreciation and thanks, the many collaborators that have played key roles in our work along these directions over the years: K. Krischer, M. Graham, J. Lauterbach, K.Asakura, M. Baer, A. Bangia, J. Krishnan, G. Haas, J. Wolff, Prof. Ronald Imbihl and his students N. Hartmann and E. Schuetz, Prof. S. Y. Shvartsman, who started these ignition studies in his Thesis, as well as M. Lange (Sensors Unlimited) for many a sample preparation. This work would not happen without G. Ertl, whose inspiration, guidance and constant encouragement it is a pleasure to acknowledge.

REFERENCES

[1] A. Uppal. W. H. Ray and A. B. Poore, "Dynamic behavior of continuous stirred tank reactors", Chem. Eng. Sci. **29**(40), 967-985 (1974).

[2] K. F. Jensen and W. H. Ray, "The bifurcation behavior of tubular reactors", Chem. Eng. Sci. **37**(2), 199-222 (1982).

[3] Y. S. Matros and G. A. Bunimovich, "Reverse-flow operation in fixed bed catalytic reactors", Cat. Rev. **38**, 1-68 (1996).

[4] Yu. Suchorski, J. Beden, E.W. James, J.W. Evans and R. Imbihl, "Fluctuation-induced transitions in a bistable surface reaction: catalytic CO oxidation on a Pt Field Emitter Tip", Phys. Rev. Lett. **82**, 1907-1910 (1999).

[5] H.-C. Chang, "The domain model for heterogeneous catalysis", Chem. Eng. Sci. **38**(4), 535-546 (1983).

[6] P. C. Pawlicki and R. A. Schmitz, "Spatial effects on supported catalysts", Chem. Eng. Sci. **83**(2), 40-45 (1987).

[7] J. P. Keener, "Homogenization and propagation in the bistable equation", Physica D **136**, 1-17 (2000).

[8] J. P. Keener, "Propagation of Waves in an Excitable Medium with Discrete Release Sites", SIAM J. Appl. Math. **61**, 317-334 (2000).

[9] A. T. Winfree, "Evolving perspective during 12 years of electrical turbulence", Chaos **8**, 48-55 (1998).

[10] A. V. Panfilov and J. P. Keener, "Re-entry in an anatomical model of the heart", Chaos Solitons Fract. **5**, 681-689 (1995).

[11] J. M. De Santos, T. R. Melli and L. E. Scriven, "Mechanics of gas-liquid flow in packed-bed contactors", Annu. Rev. Fluid Mech. **23**, 233-260 (1991).

[12] D. G. Avraam and A. C. Payatakes, "Flow Regimes and Relative Permeabilities during Steady-State Two-Phase Flow in Porous Media", J. Fluid Mech. **293**, 181-206 (1995).

[13] M. D. Graham, I. G. Kevrekidis, K. Asakura, J. Lauterbach, K. Krischer, H. H. Rotermund and G. Ertl, "Effects of boundaries on pattern formation: catalytic oxidation of CO on Platinum", Science **264**, 80-82 (1994).

[14] H.H. Rotermund, W. Engel, M. Kordesch and G. Ertl, "Imaging of spatiotemporal pattern evolution during carbon-monoxide oxidation on platinum" Nature **343**, 355-357 (1990).

[15] N. Hartmann, M. Bär, I. G. Kevrekidis K. Krischer and R. Imbihl, "Rotating chemical waves in small circular domains", Phys. Rev. Lett. **76**(8), 1384-1387 (1996).

[16] G. Haas, M. Bär, I. G. Kevrekidis, H. H. Rotermund and G. Ertl, "Observation of Front bifurcations in controlled geometry: From one to two dimensions", Phys. Rev. Lett. **75**(19), 3560-3563 (1995).

[17] J. Christoph, M. Eiswirth, N. Hartmann, R. Imbihl, I. G. Kevrekidis and M. Bär, "Anomalous dispersion and pulse interaction in an exitable surface reaction", Phys. Rev. Lett. **82**, 1586-1589 (1999).

[18] J. Krishnan, K. Engelborghs, M. Bär, K. Lust, D. Roose, and I. G. Kevrekidis, "A computer-assisted study of pulse dynamics in anisotropic media", Physica D **154**, 85-110 (2001).

[19] J. D. Crawford, J. P. Gollub, and D. Lane, "Hidden symmetries of parametrically forced waves", Nonlinearity **6**, 119-164 (1993).

[20] O. Steinbock, P. Kettunen and K. Showalter, "Anisotropy and spiral organizing centers in patterned excitable media", Science **269**(29), 1857-1860 (1995).

[21] A. L. Lin, M. Bertram, K. Martinez, H. L. Swinney, A. Ardelea, and G. F. Carey, "Resonant Phase Patterns in a Reaction-Diffusion System", Phys. Rev. Lett. **84**, 4240-4243

(2000).

[22] K. Agladze, J. P. Keener, S. C. Müller and A. Panfilov, "Rotating Spiral waves created by geometry", Science **264**, 1746-1748 (1994).

[23] A. Lázár, Z. Noszticzius, H. Farkas and H. D. Forsterling, "Involutes: the geometry of chemical waves rotating in annular membranes", Chaos **5**(2), 443-447 (1995).

[24] K. Suzuki, T. Yoshinobu and H. Iwasaki, "Diffusive Propagation of chemical waves through a microgap", J. Phys. Chem. A **104**, 5154-5159 (2000).

[25] R. Srinivasan, I. M. Hsing, P. E. Berger, K. F. Jensen, S. L. Firebaugh, M. A. Schmidt, M. P. Harold, J. J. Lerou and J. F. Ryley, "Micromachined reactors for catalytic partial oxidation reactions", AIChE J. **43**, 3059-3069 (1997).

[26] H. Loewe and W. Ehrfeld, "State-of-the-art in microreaction technology: concepts, manufacturing and applications", Electrochimica Acta. **44**, 3679-3689 (1999).

[27] K. Asakura, J. Lauterbach, H. H. Rotermund and G. Ertl, "Spatio-temporal pattern formation during catalytic CO oxidation on a Pt(100) surface modified with submonolayer of Au", Surf. Sci. **374**, 125-141 (1997).

[28] E. Schütz, N. Hartmann, I. G. Kevrekidis and R. Imbihl, "Catalysis on microstructured surfaces", Faraday Disc. **105**, 47-56 (1996).

[29] F. Esch, S. Günther, E. Schütz, A. Schaak, I. G. Kevrekidis, M. Marsi, M. Kiskinova and R. Imbihl, "Chemically resolved dynamical imaging of catalytic reactions on composite surfaces", Catalysis letters **52**, 85-90 (1998).

[30] E. Schütz, N. Hartmann, I.G. Kevrekidis and R. Imbihl, "Microchemical engineering of catalytic reactions, Catalysis letters **54**, 181-186 (1998).

[31] F. Esch, S. Günther, E. Schütz, A. Schaak, I. G. Kevrekidis, M. Marsi, M. Kiskinova and R. Imbihl, "Chemical waves and adsorbate-induced segregation on a Pt(100) surface

microstructured with a thin Rh/Pt film", Surf. Sci. **443**, 245-252 (1999).

[32] M. Pollmann, H. H. Rotermund, G. Ertl, X. Li and I.G. Kevrekidis, "Formation of 2-d concentration pulses on microdesigned composite catalyst surface", Phys. Rev. Letters **86**, 6038-6041 (2001).

[33] J. Lauterbach, K. Asakura, P. B. Rasmussen, H. H. Rotermund, M. Bär, M. D. Graham, I. G. Kevrekidis and G. Ertl, "Catalysis on mesoscopic composite surfaces: Influence of Pd boundaries on pattern formation during CO-oxidation on Pt(110)", Physica D **123**, 493-501 (1998).

[34] J. P. Voroney, A. T. Lawniczak and R. Kapral "Turing Pattern formation in heterogeneous media", Physica D **99**, 303-317 (1996)

[35] M. A. Liauw, J. Ning and D. Luss. "Pattern formation on a nonuniformly active ring", J. Chem. Phys. **104**, 5657-5662 (1996)

[36] A. Lázár, H. D. Försterling, H. Farkas, P. Simon , A. Volford and A. Noszticzius, "Waves of excitation on nonuniform membrane rings, caustics, and reverse involutes", Chaos **7**, 731-737 (1997)

[37] M. D. Graham, M. Bär, I. G. Kevrekidis, K. Asakura, J. Lauterbach, K. Krischer, H. H. Rotermund and G. Ertl, "Catalysis on a microstructured surfaces: Pattern formation during CO oxidation in complex Pt domains", Phys. Rev. E **32**(1), 76-93 (1995).

[38] M. Bär, I. G. Kevrekidis, H. H. Rotermund and G. Ertl, "Pattern formation in composite excitable media", Phys. Rev. E **52**(6), 5739-5742 (1995).

[39] A. K. Bangia, M. Bär, I. G. Kevrekidis, M. D. Graham, H. H. Rotermund and G. Ertl, "Catalysis on microcomposite surfaces", Chem. Eng. Sci. **51**(10), 1757-1765 (1996).

[40] M. Bär, A. K. Bangia, I. G. Kevrekidis, G. Haas, H. H. Rotermund and G. Ertl, "Composite catalyst surfaces: effect of inert and active heterogeneities on pattern formation",

J. Phys. Chem. **100**(49), 19106-19117 (1996).

[41] M. G. Zimmermann, S. O. Firle, M. A. Natiello, M. Hildebrand, M. Eiswirth, M. Bär, A. K. Bangia and I. G. Kevrekidis, "Pulse bifurcation and transition to spatiotemporal chaos in an excitable reaction-diffusion model", Physica D **110**, 92-104 (1997).

[42] S. Y. Shvartsman, E. Schütz, R. Imbihl and I. G. Kevrekidis, "Dynamics on microcomposite catalytic surfaces: The effect of active boundaries", Phys. Rev. Lett. **83**, 2857-2860 (1999); Erratum, Phys. Rev. Lett. **85**, 902 (2000).

[43] N. Hartmann, I. G. Kevrekidis and R. Imbihl, "Pattern formation in restricted geometries: the NO +CO reaction on Pt(100)", J. Chem. Phys. **112**, 6795-6803 (2000).

[44] S. Y. Shvartsman, E. Schütz, R. Imbihl and I. G. Kevrekidis, "Dynamics of catalytic reactions on microdesigned surfaces", Catalysis Today **70**, 301-310 (2001).

[45] S. Y. Shvartsman, *Dynamics and control of reaction-diffusion systems*, Thesis (Princeton University, 1999).

[46] M. X. Yang, D. H. Gracias, P. W. Jacobs and G. A. Somorjai: "Lithographic fabrication of model systems in heterogeneous catalysis and surface science studies", Langmuir **14** 1458-1464 (1998).

[47] R.E.R. Colen, M. Kolodziejczyk, B. Delmon and J. H. Block: "Kinetic study of CO oxidation on copper modified Pt(111)" Surface Science **413** 447-457 (1998).

[48] P. De Kepper, E. Dulos, J. Boissonade, A. De Wit,G. Dewel and P. Borckmans, "Reaction-diffusion patterns in confined chemical systems", J. Stat. Phys. **101**, 495-508 (2000).

[49] K. Suzuki, T. Yoshinobu and H. Iwasaki, "Unidirectional propagation of chemical waves through microgaps between zones with different excitability", J. Phys. Chem. A **104**, 6602-6608 (2000).

[50] J. Wolff, T. Papathanasiou, I. G. Kevrekidis, H. H. Rotermund and G. Ertl, "Spatio-

temporally addressing surface activity", Science, **294**, 134-137 (2001).

[51] V. Petrov, V. Gaspar, J. Masere and K. Showalter, "Controlling chaos in the Belousov-Zhabotinsky reaction", Nature **361**, 240-263 (1993).

[52] M. Kim, M. Bertram, M. Pollmann, A. V. Oertzen, A. S. Mikhailov, H. H. Rotermund and G. Ertl, "Controlling chemical chaos by global delayed feedback: pattern formation in catalytic CO oxidation on Pt(110)" Science **292**, 1357-1360 (2001).

[53] K. Krischer, M. Eiswirth and G. Ertl, "Oscillatory CO oxidation on Pt(110): Modeling of temporal self-organization", J. Chem. Phys. **96**, 9161-9172 (1992)

[54] M. Bär, N. Gottschalk, M. Eiswirth and G. Ertl, "Spiral waves in a surface reaction: Model calculations", J. Chem. Phys. **100**, 1202-1214 (1994)

[55] R. B. Lehoucq, D. C. Sorensen and C. Yang. *ARPACK Users' Guide*, (SIAM, Philadelphia, 1998)

[56] F. Mertens and R. Imbihl, "Square Chemical Waves in the catalytic reaction NO + H_2 on a Rhodium (110) surface" Nature **370**, 124-126 (1994).

[57] M. Bär, A. Hagberg, E. Meron and U. Thiele, "Front propagation and pattern formation in anisotropic bistable media", Phys. Rev. E **62**, 366 (2000).

[58] A. Bensoussan, J. -L. Lions and G. Papanicolaou, *Asymptotic methods for periodic structures* (McGraw-Hill, New York, 1978).

[59] J. Xin, "Front propagation in heterogeneous media", SIAM Rev. **42**(2), 161-230 (2000)

[60] T. -Y. Hou and X.-H. Wu. "A multiscale finite element method for elliptic problems in composite materials and porous media", J. Comput. Phys. **134**, 169-189 (1997).

[61] T. Y. Hou, X.-H. Wu and Z. Cai. "Convergence of a multiscale finite element method for elliptic problems with rapidly oscillating coefficients", Math. Comp. **68**, 913–943 (1999).

[62] V. B. Shenoy, R. V. Kukta and B. Phillips, “Mesoscopic analysis of structure and strength of dislocation junctions in FCC Metals”, Phys. Rev. Lett. **84**, 1491-1494 (2000).

[63] G. Beylkin and M. Brewster. “A multiresolution strategy for numerical homogenization”, Appl. Comput. Harmon. Anal. **2**, 327-349 (1995).

[64] M. Dorobantu and B. Engquist. “Wavelet-based numerical homogenization”, SIAM J. Numer. Anal. **35**, 540-559 (1998).

[65] A. C. Gilbert. “A comparison of multiresolution and classical one-dimensional homogenization schemes”, Appl. Comput. Harmon. Anal. **5**, 1-35 (1998).

[66] J. Krishnan, O. C. Runborg and I. G. Kevrekidis, “Application of wavelet-based reduction techniques to nonlinear reaction-transport problems”, Nonlinearity, **in press** (2002).

[67] P. G. Kevrekidis and I.G. Kevrekidis, “Pattern speed reduction in heterogeneous 1d Reaction-diffusion systems”, Proceedings of 13th conference on “Nonlinear dynamics, chaos and complexity”, Chania, Greece, submitted (2001).

[68] P. G. Kevrekidis, I. G. Kevrekidis and A.R. Bishop, “Propagation failure, universal scalings and Goldstone modes”, Phys. Lett. A, **279**, 361 (2001).

[69] P. G. Kevrekidis and I.G. Kevrekidis “Heterogeneous vs. discrete mapping problem”, Phys. Rev. E., **64** 056624(1-8) (2001)

[70] O. Runborg, C. Theodoropoulos and I.G. Kevrekidis, “Effective stability and bifurcation analysis: a time stepper based approach”, Nonlinearity, in press (2002).

[71] M. Park, C. Harrison, P. M. Chaikin, R. A. Register and D. H. Adamson, “Block copolymer lithography: periodic Arrays of 10^{11} holes in 1 square centimeter”, Science **276**, 1401-1404 (1997).

[72] M. Böltau, S. Walheim, J. Mlynek, G. Krausch and U. Steiner, “Surface-induced structure formation of polymer blends on patterned substrates”, Nature **391**, 877-879 (1998).

[73] P. Shah, I.G. Kevrekidis and J.B. Benziger, "Ink-jet printing of catalyst patterns for electroless metal deposition", Langmuir **15**, 1584-1587 (1999).

[74] C. S. Chen, M. Mrksich, S. Huang, G. M. Whitesides and D. E. Ingber, "Geometric control of cell life and death", Science **276**, 1425-1428 (1997).

[75] R. S. Kane, S. Takayama, E. Ostuni, D. E. Ingber, G. M. Whitesides, "Patterning proteins and cells using soft lithography", Biomaterials **20**, 2363-2376 (1999).

[76] R.C. Hayward, D. A. Saville and I. A. Aksay, "Electrophoretic Assembly of Colloidal Crystals with Optically Tunable Micropatterns", Nature **405**, 56-59 (2000).

FIGURES

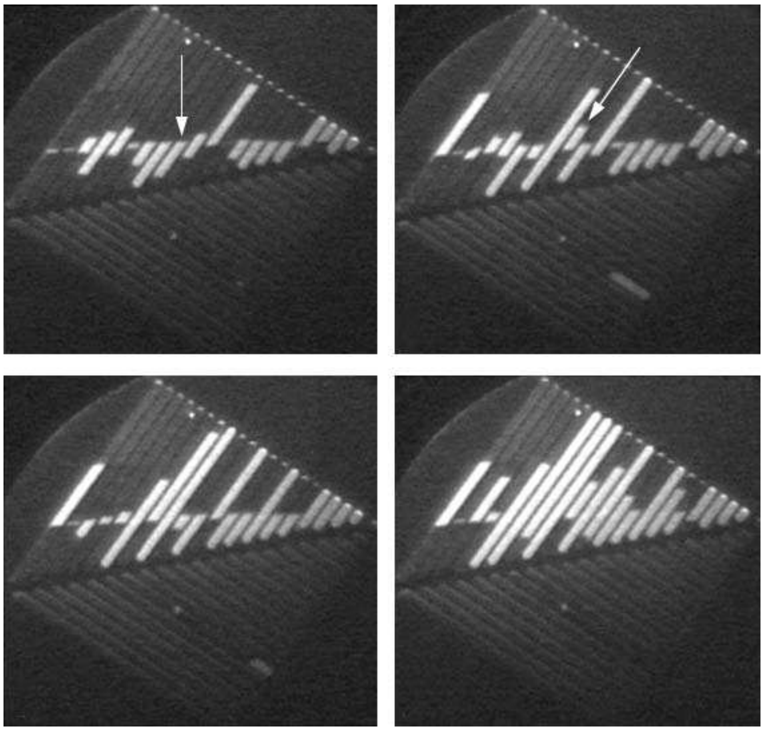

FIG. 1. "Inert walls": PEEM image showing CO fronts during CO oxidation in $20\mu m$ wide Pt channels, separated by Ti barriers. Front initiation occurs at a crystal imperfection (a scratch, marked by an arrow in the top left panel). Experimental conditions: $P_{CO} = 2.3 * 10^{-5}$mbar, $P_{O_2} = 4 * 10^{-4}$mbar, $T = 420$K

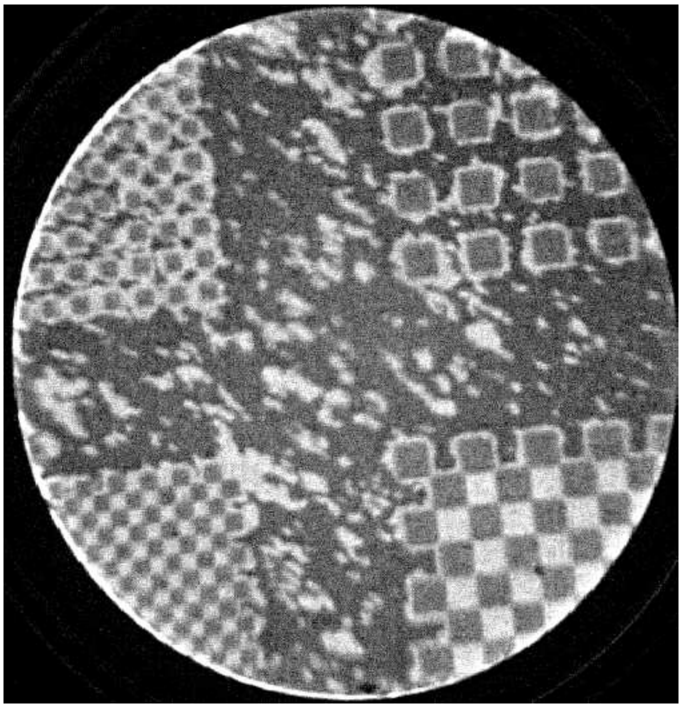

FIG. 2. Composite catalysts: lattices of Rh inclusions on a Pt single crystal surface. Notice how the size and geometry of the inclusions affects what occurs on the Pt "within" the lattice, as well as the "open" Pt in the cross-shaped area at the center. Rh squares: 50 and 100 microns size.

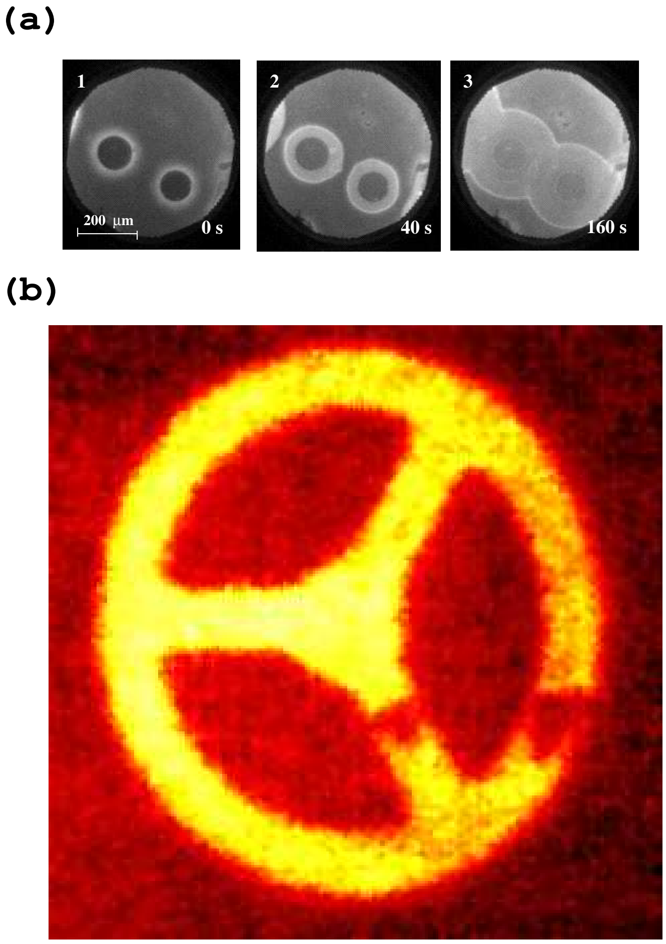

FIG. 3. (a) A Pt(100)/Rh composite surface (the dark, circular inclusions are Pt). Upon increase of P_{H_2} from $2 * 10^{-6}$ to $7 * 10^{-6}$mbar for the $NO + H_2$ reaction, a reactive front initiation (ignition) at the boundary between the two active components is observed. Experimental conditions: $P_{NO} = 2 * 10^{-6}$mbar, $T = 437$K. (b)"Leaky walls": PEEM image showing triangular oxygen pulses travelling in the corridors of a three-spoked Pt wheel construction surrounded by Rh. CO oxidation at $P_{CO} = 3.3 * 10^{-5}$mbar. $P_{O_2} = 4 * 10^{-4}$mbar, $T = 435$K. The triangular shape is believed to be due to the surface diffusion of adsorbed CO from the Rh across the corridor boundary to the Pt.

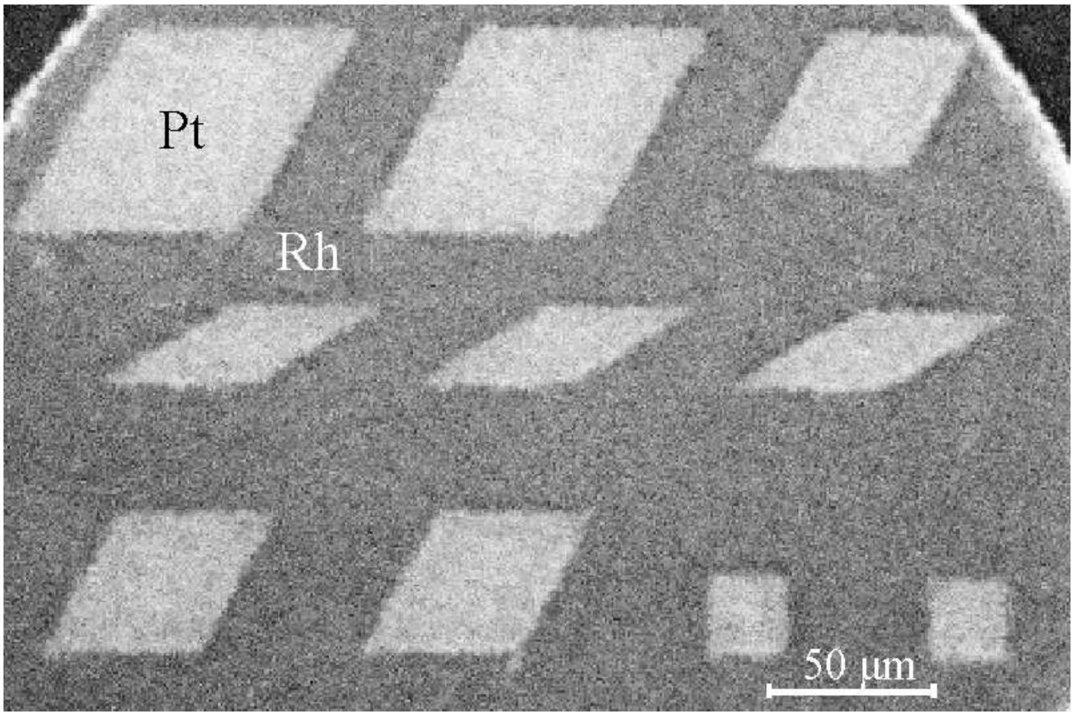

, width=3.5inch

FIG. 4. Microphotograph of the composite catalyst Pt/Rh used in the experiments.

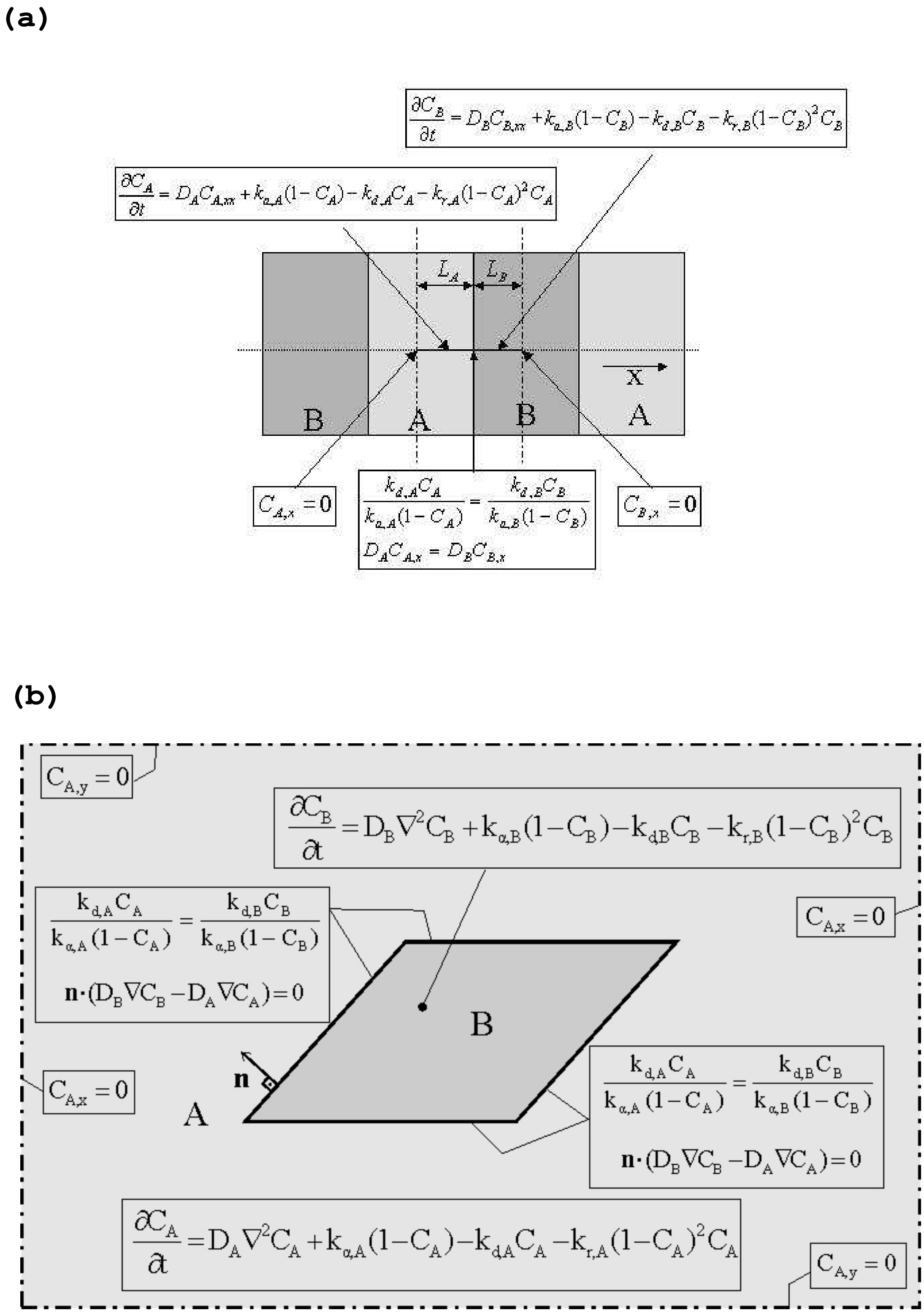

FIG. 5. Schematic of the model equations, geometry and boundary conditions used in one and in two dimensional simulations.

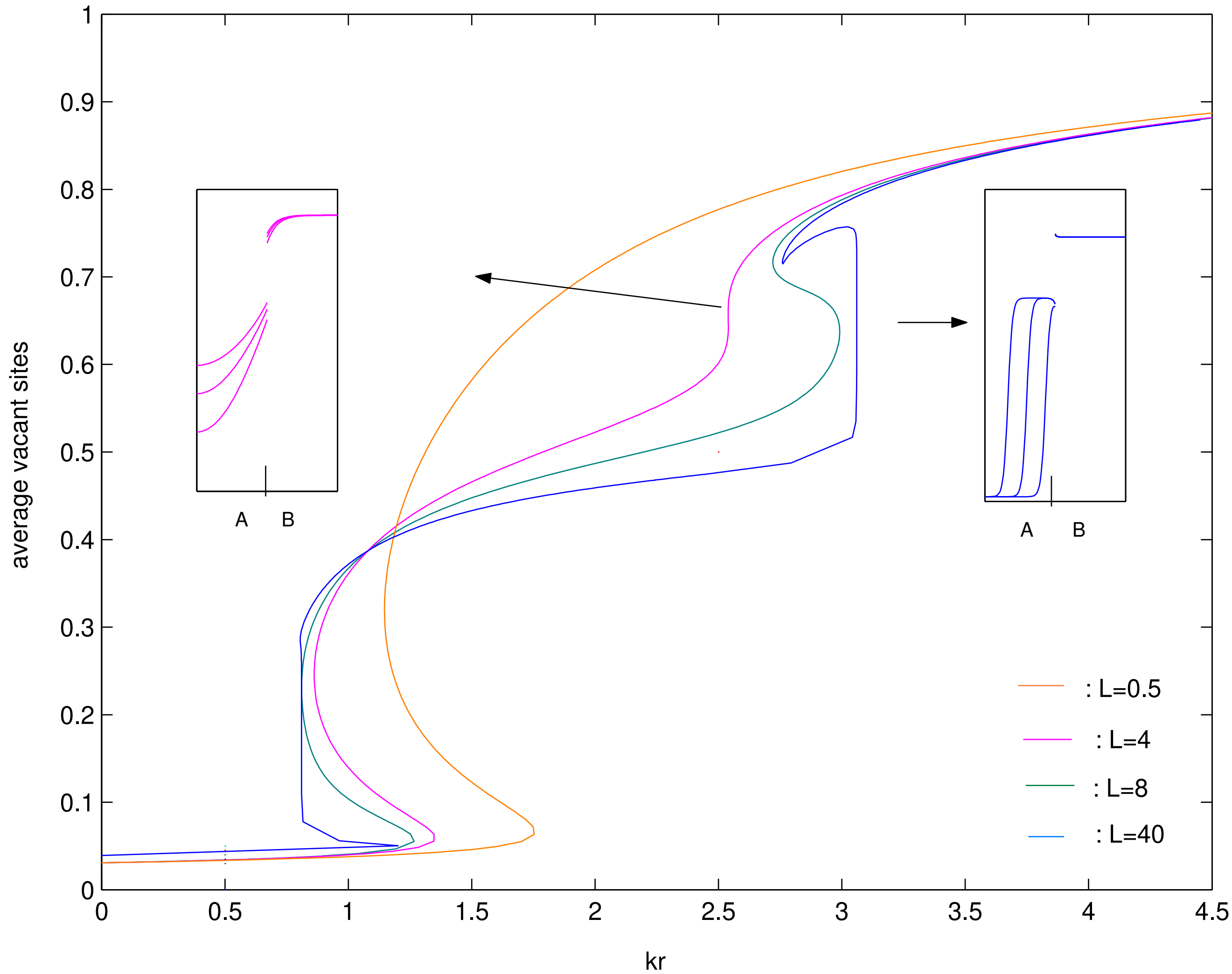

FIG. 6. Bifurcation diagram for "50-50" composite striped media ($L_A = L_B = L$), $D_A = D_B = 1$ at different stripe widths L. Here $k_{aA/B} = 0.7/0.4$; $k_{dA/B} = 0.01/0.02$; $k_{rB} = 2 * k_{rA}$, and $k_{rA} = k_r$, our bifurcation parameter. Inset on the right: spatial profiles of solutions on the vertical branch for $L = 40$. Inset on the left: spatial profiles of solutions on the counterpart vertical branch of the bifurcation diagram for $L = 4$.

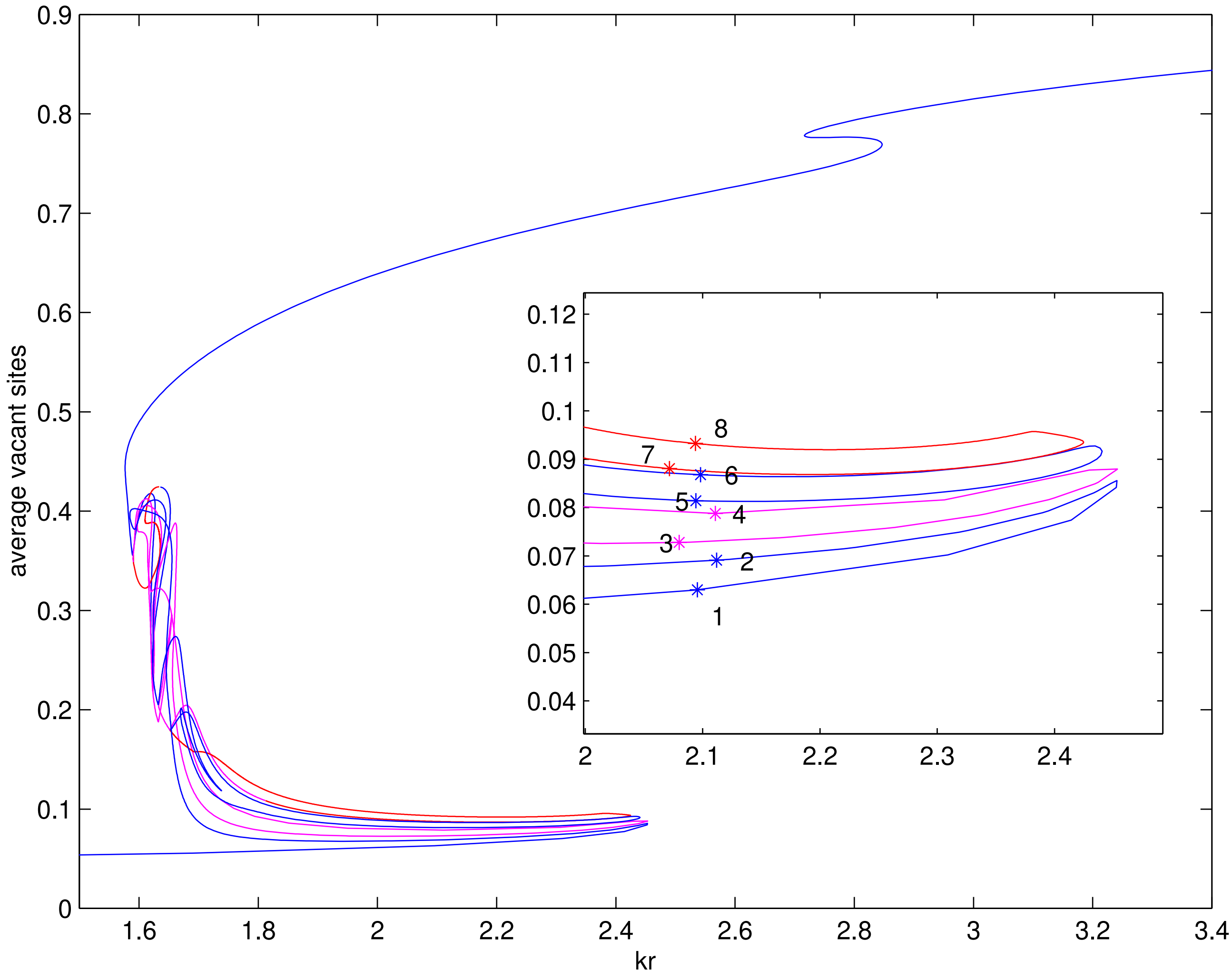

FIG. 7. Bifurcation diagram of a composite surface: B (more active) is the complement the rhomb. Here the unit square cell $L = 45$; the area of the rhomb is 225; the rhomb angle is 60°; $D_A = D_B = 1$; $k_{aA/B} = 0.7/0.4$; $k_{dA/B} = 0.01/0.02$; $k_{rB} = 2 * k_{rA}$, and $k_{rA} = k_r$.

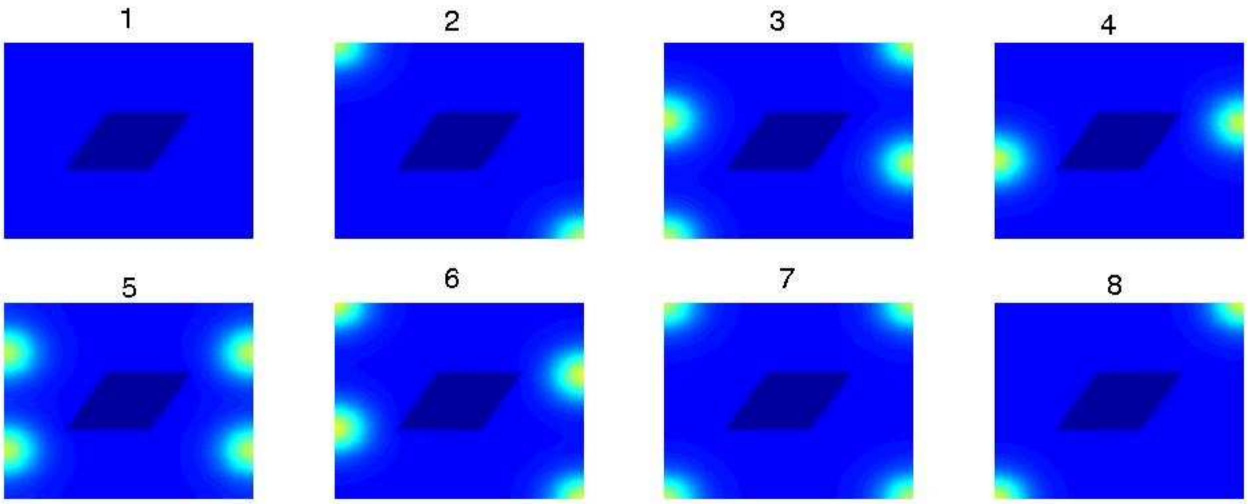

FIG. 8. The steady state solution contours corresponding to the marked points in Fig. 7

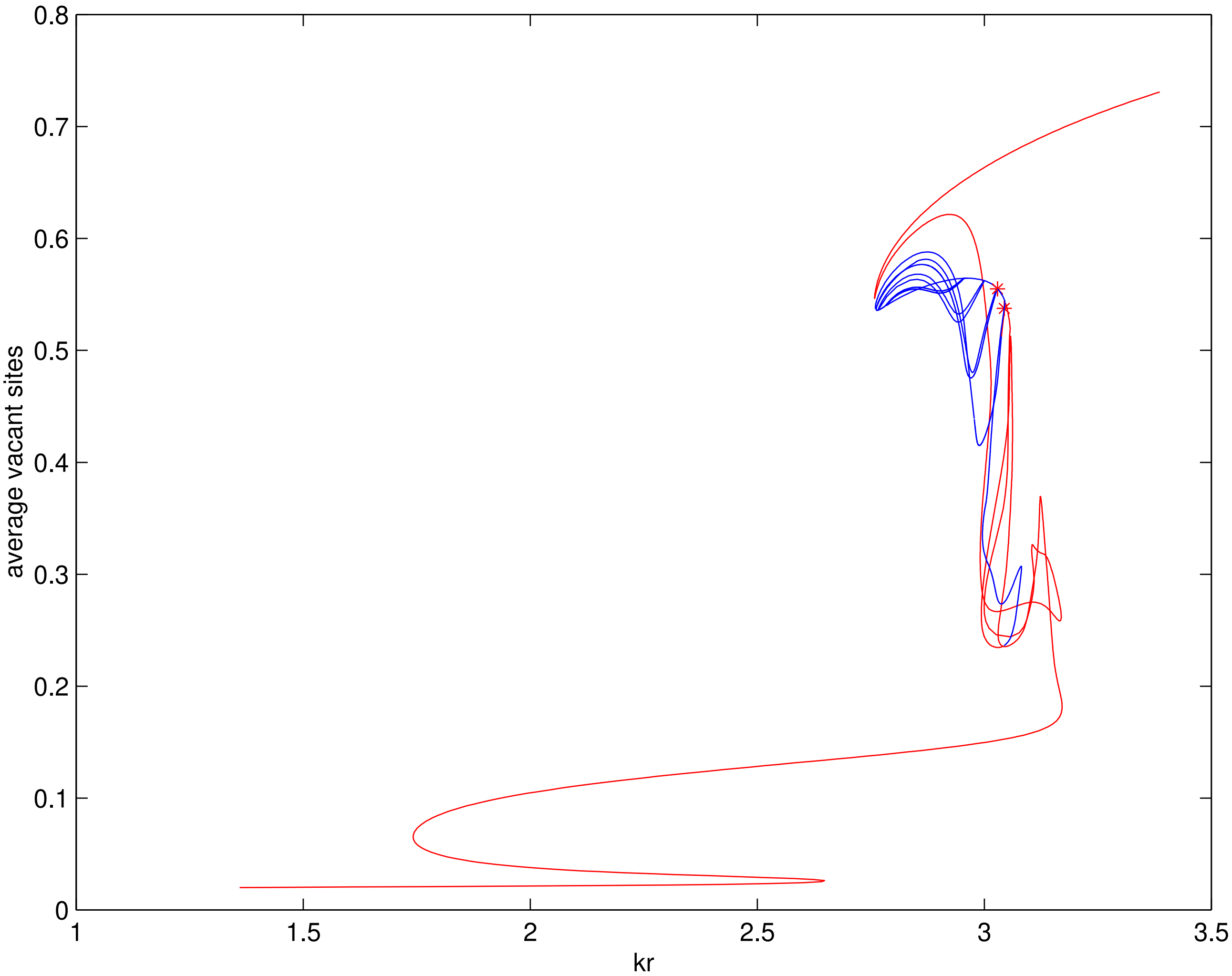

FIG. 9. Bifurcation diagram of a composite surface: B (more active) is inside the rhomb. Here the unit square cell $L = 45$; the area of the rhomb is 225; the rhomb angle is $60°$; $D_A = D_B = 1$; $k_{aA/B} = 0.7/0.4$; $k_{dA/B} = 0.01/0.02$; $k_{rB} = 2 * k_{rA}$, and $k_{rA} = k_r$.

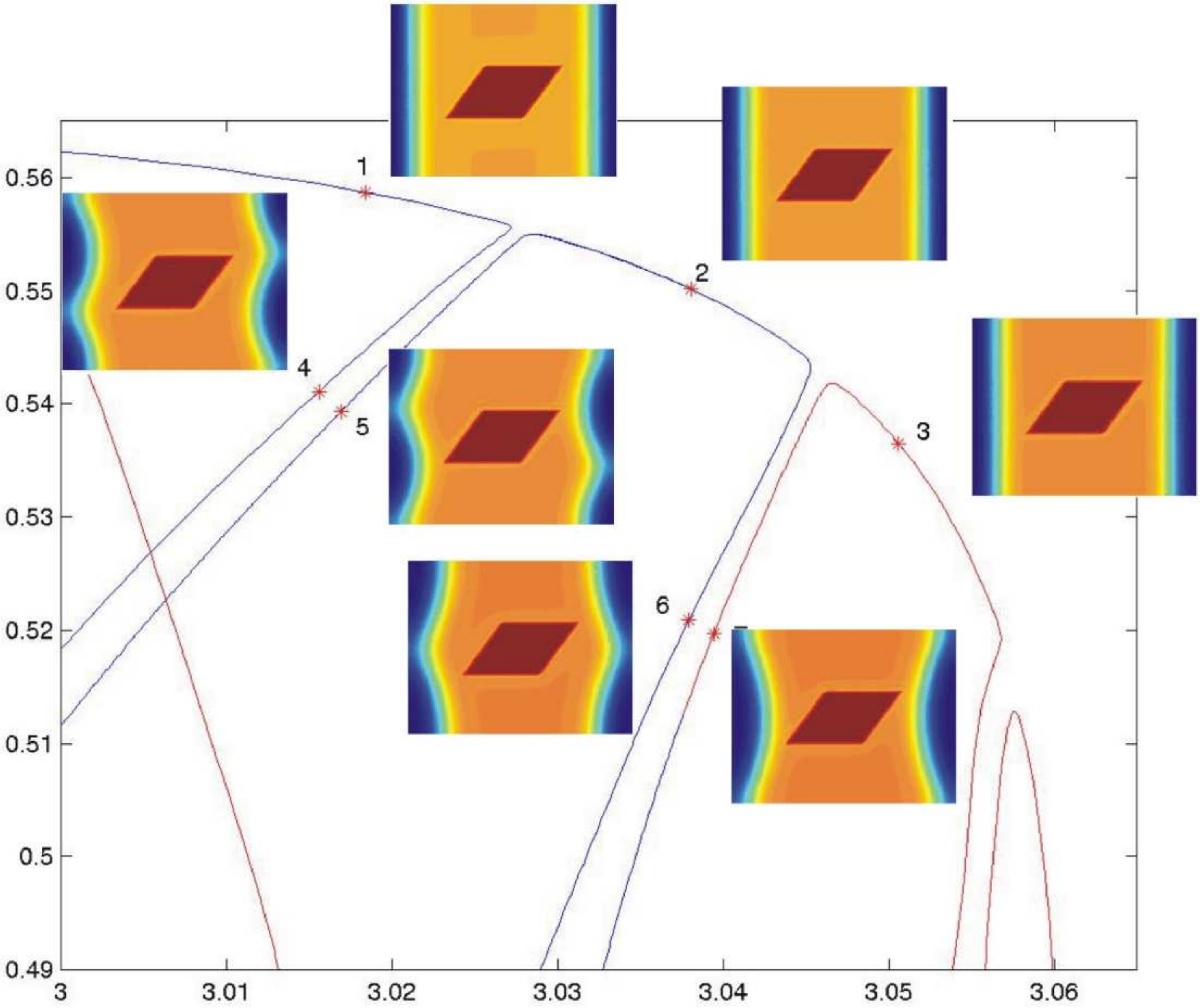

FIG. 10. A blow-up of Fig. 6 with steady state contours; notice the several perturbed pitchfork bifurcations.

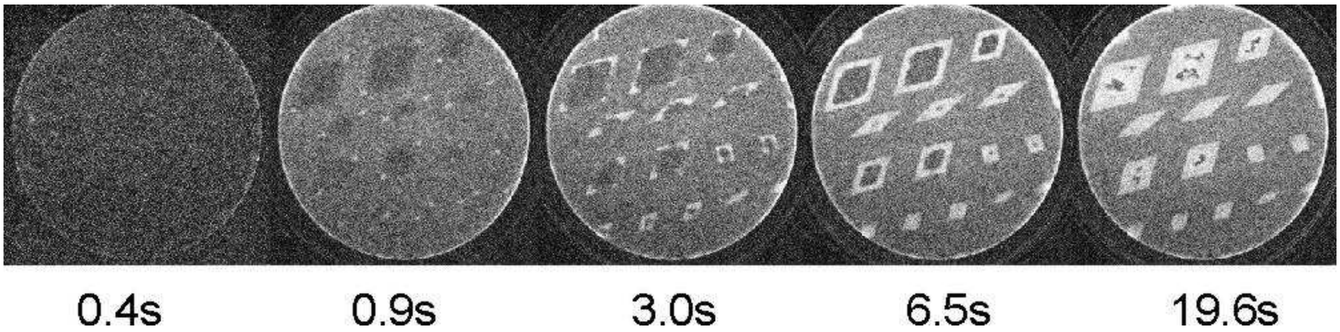

FIG. 11. PEEM image showing transient ignition for various Pt rhomb inclusions in Rh after a "jump" in the P_{CO} from 0 to $3 * 10^{-6}$mbar. Other experimental conditions: $P_{O_2} = 4 * 10^{-4}$mbar, $T = 460$K

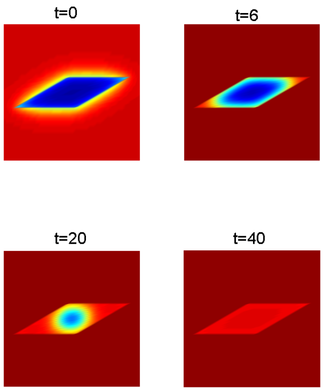

FIG. 12. Simulation results showing transient ignition following a step change of k_r from 1.7 to 3.0. Here the unit square cell $L = 45$; the area of the rhomb is 225; the rhomb angle is 30°; $D_A = D_B = 1$; $k_{aA/B} = 0.7/0.4$; $k_{dA/B} = 0.01/0.02$; $k_{rB} = 2 * k_{rA}$, and $k_{rA} = k_r$.

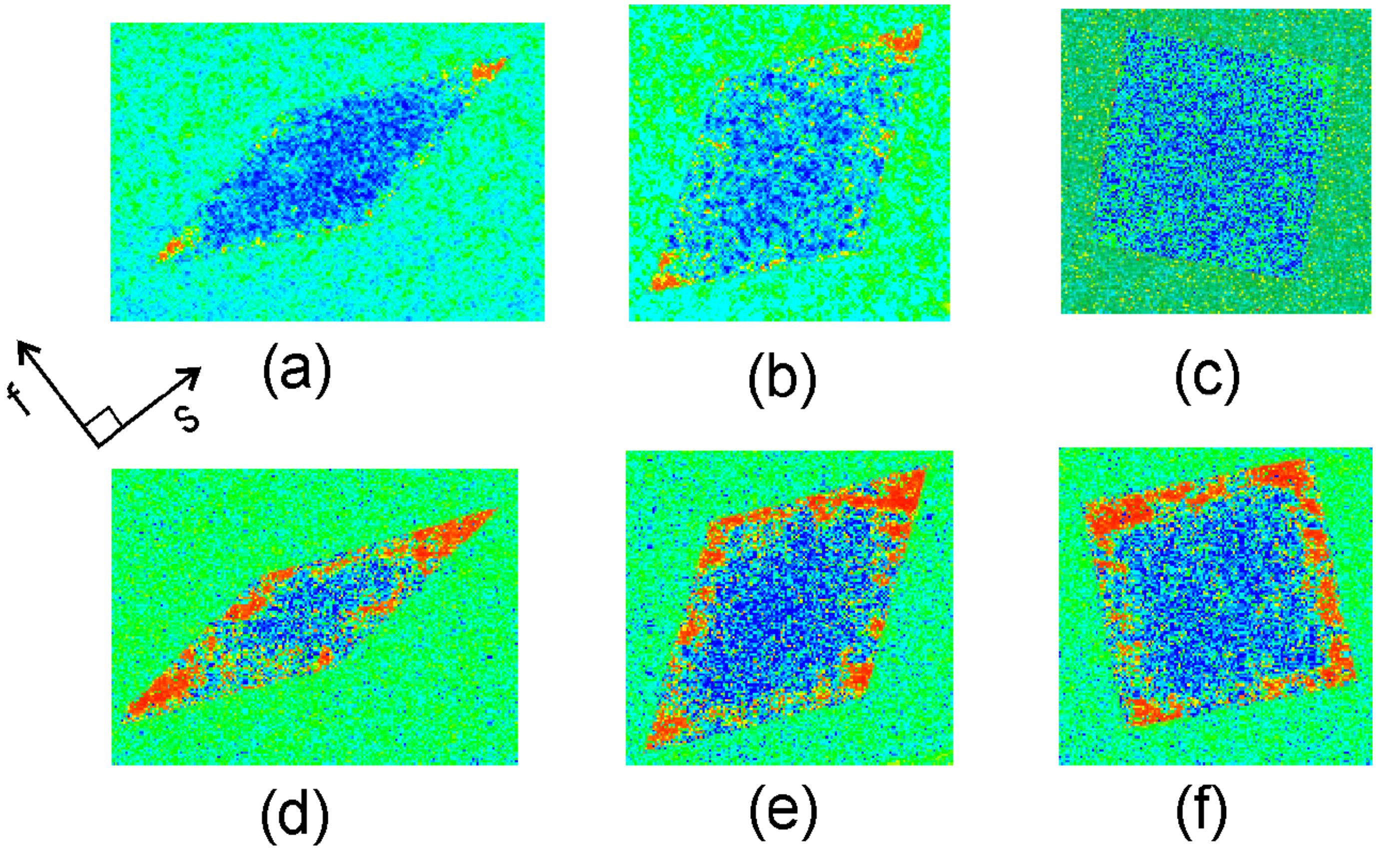

FIG. 13. The effect of angle and CO pressure on CO front nucleation: the steady states shown in the first row are obtained at $P_{CO} = 1.5 * 10^{-5} mbar$; the second row was obtained at $P_{CO} = 2.5 * 10^{-5} mbar$; $P_{O_2} = 4 * 10^{-4} mbar$, $T = 458K$ for both experiments. f and s denote the fast and slow diffusion axes along the anisotropic surface.

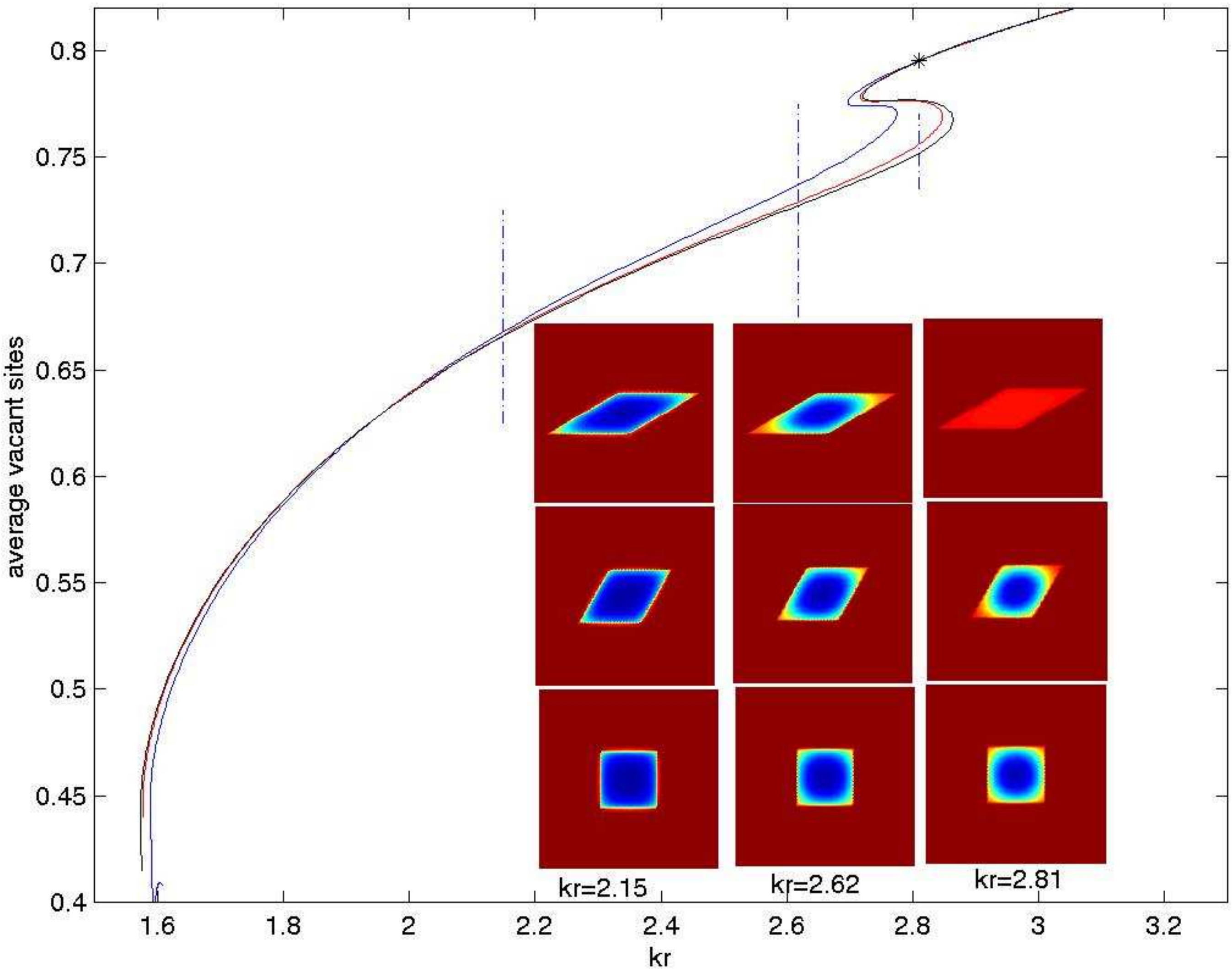

FIG. 14. Bifurcation diagram and steady state contours for rhombs at different angles: 30°, 60°, 90°. Here the unit square cell $L = 45$; the area of the rhomb is 225; $D_A = D_B = 1$; $k_{aA/B} = 0.7/0.4$; $k_{dA/B} = 0.01/0.02$; $k_{rB} = 2 * k_{rA}$, and $k_{rA} = k_r$. Notice that the sharpest rhomb is completely ignited at $k_r = 2.81$.

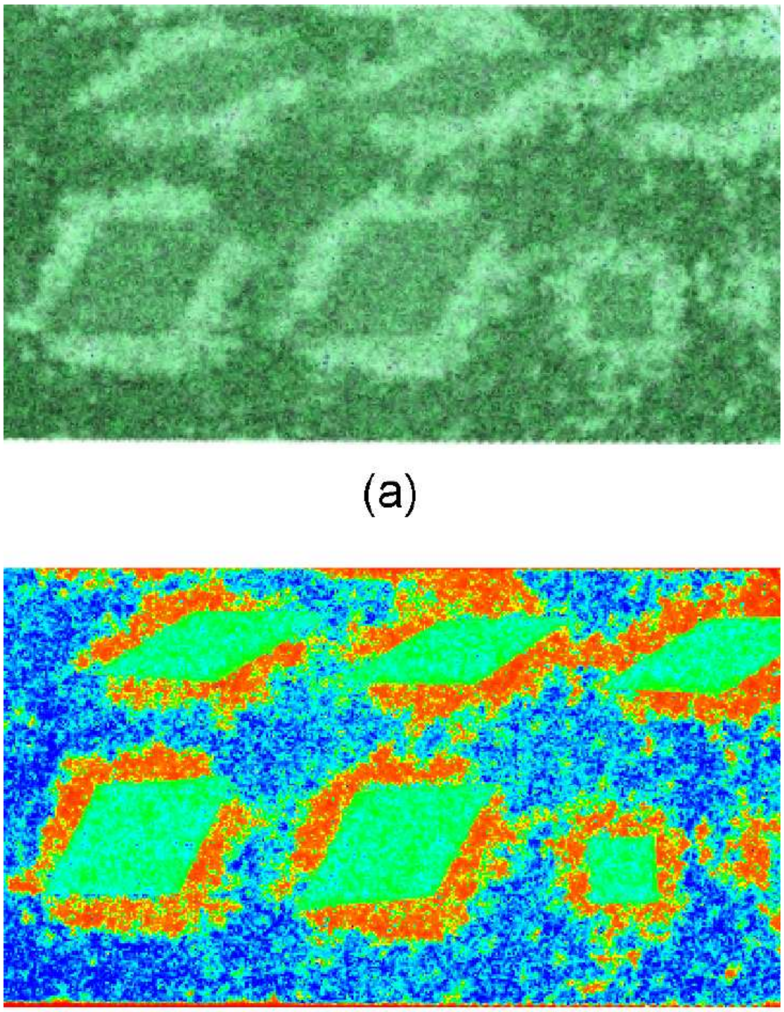

(a)

(b)

FIG. 15. CO front nucleation around an active inclusion. The catalytic surface consists of Rh rhomb inclusions in Pt. (a) raw experimenal image and (b) its pseudocolor enhancement. Experimental conditions: $P_{CO} = 2.5 * 10^{-5} mbar$; $P_{O_2} = 4 * 10^{-4} mbar$; $T = 458K$.

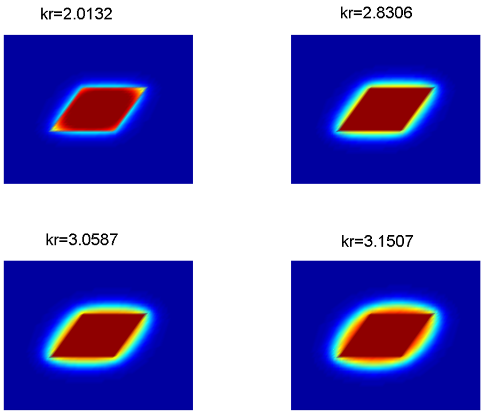

FIG. 16. Simulation: "ignited" steady state contours at different k_r. The more active B is inside the rhomb. Here the unit square cell $L = 45$; the area of the rhomb is 225; the angle of the rhomb is $60°$; $D_A = D_B = 1$; $k_{aA/B} = 0.7/0.4$; $k_{dA/B} = 0.01/0.02$; $k_{rB} = 2 * k_{rA}$, and $k_{rA} = k_r$.

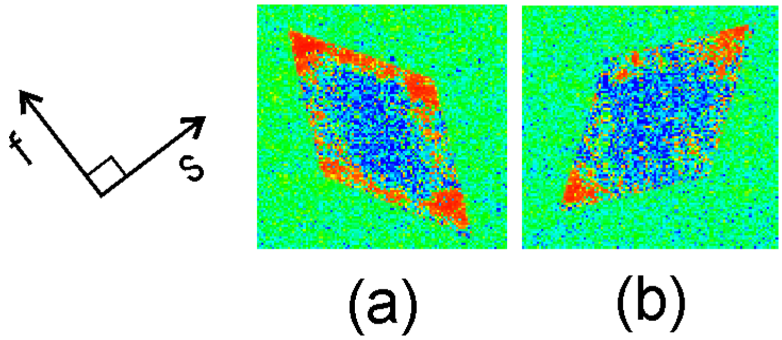

FIG. 17. The effect of anisotropy on the CO front nucleation at a rhomb angle of $60°$. f and s denote the fast and slow diffusion directions on the anisotropic crystal. Experimental conditions: $P_{CO} = 2.3 * 10^{-5} mbar$; $P_{O_2} = 4 * 10^{-4} mbar$; $T = 458K$.